AB

DPNU 93-28

jle 9409

DPNU-93-28
KEK Preprint 93-74
TUAT-HEP 93-04
TIT-HPE-93-07
NWU-HEP 93-05
OCU-HEP 93-06
KOBE-HEP 93-08
PU-93-671
INS-REP-998
TU-HEP 93/03

Measurement of the forward-backward asymmetry of $e^+e^- \to c\bar{c}$ at $\sqrt{s}$=57.95 GeV*

TOPAZ Collaboration

E.Nakano[a], R.Enomoto[b], K.Abe[c], T.Abe[a], I.Adachi[b], M.Aoki[a], S.Awa[d], R.Belusevic[b], K.Emi[c], H.Fujii[b], K.Fujii[b],T.Fujii[e], J.Fujimoto[b], K.Fujita[f], N.Fujiwara[d], H.Hayashii[d], B.Howell[g], N.Iida[b], H.Ikeda[b], R.Itoh[b], H.Iwasaki[b], M.Iwasaki[d], R.Kajikawa[a], S.Kato[h], S.Kawabata[b], H.Kichimi[b], M.Kobayashi[b], D.Koltick[g], I.Levine[g], K.Miyabayashi[a], A.Miyamoto[b], K.Muramatsu[d], K.Nagai[i], T.Nagira[d], N.Nakabayashi[a], O.Nitoh[c], S.Noguchi[d], F.Ochiai[j], Y.Ohnishi[a], H.Okuno[h], T.Okusawa[f], K.Shimozawa[a], T.Shinohara[c], A.Sugiyama[a], N.Sugiyama[k], S.Suzuki[a], K.Takahashi[c], T.Takahashi[f], M.Takemoto[d], T.Tanimori[k], T.Tauchi[b], F.Teramae[a], Y.Teramoto[f], N.Toomi[d], T.Toyama[a], T.Tsukamoto[b], S.Uno[b], Y.Watanabe[k], A.Yamaguchi[d], A.Yamamoto[b],and M.Yamauchi[b]

* submitted to Phys. Lett. B.

(a) Department of Physics, Nagoya University, Nagoya 464, Japan
(b) KEK, National Laboratory for High Energy Physics, Ibaraki-ken 305, Japan
(c) Department of Applied Physics, Tokyo Univ. of Agriculture and Technology, Tokyo 184, Japan
(d) Department of Physics, Nara Women's University, Nara 630, Japan
(e) Department of Physics, University of Tokyo, Tokyo 113, Japan
(f) Department of Physics, Osaka City University, Osaka 558, Japan
(g) Department of Physics, Purdue University, West Lafayette, IN 47907, USA
(h) Institute for Nuclear Study, University of Tokyo, Tanashi, Tokyo 188, Japan
(i) The Graduate School of Science and Technology, Kobe University, Kobe 657, Japan
(j) Faculty of Liberal Arts, Tezukayama University, Nara 631, Japan
(k) Department of Physics, Tokyo Institute of Technology, Tokyo 152, Japan

ABSTRACT

Measurements of the forward-backward asymmetry of $e^+e^- \to c\bar{c}$ events were carried out at a mean $\sqrt{s}$ energy of 57.95GeV at TRISTAN, KEK. The $c\bar{c}$ events were tagged either by the full-reconstruction of $D^{*\pm}$ or the inclusive P_T spectrum of $\pi_s^\pm$ from $D^{*\pm} \to D^0(\bar{D}^0)\pi_s^\pm$. The forward-backward asymmetry was measured to be $A_{FB}^c = -0.49^{+0.14}_{-0.13}(\text{stat.}) \pm 0.06(\text{sys.})$, consistent with the standard model.

1. Introduction

Measurements of the forward-backward charge asymmetry of quarks provide a good test of the standard model concerning electroweak interactions in the quark sector.[1] A number of experiments at PEP/PETRA/LEP have been performed in order to measure the forward-backward asymmetry of charm quarks by reconstructing $D^{*\pm}$ mesons at various energies.[2] Although their results were consistent with the prediction of the standard model, the statistical significance of each experiment was poor because of the low statistics and/or low asymmetry values. In the TRISTAN energy region, since the forward-backward asymmetry is approaching its maximum value, more precise measurements of electroweak interference can be expected.[3]

The TOPAZ experiment at TRISTAN (KEK) carried out measurements of the forward-backward asymmetry of charm-quark pair production identified with full- and semi-reconstructions of $D^{*\pm}$ mesons. The following decay modes were used in a full-reconstruction analysis:

$$D^{*\pm} \rightarrow \pi^{\pm} D^0(\bar{D}^0) \rightarrow \pi^{\pm} K^{\mp} \pi^{\pm}$$

$$\text{and} \quad D^{*\pm} \rightarrow \pi^{\pm} D^0(\bar{D}^0) \rightarrow \pi^{\pm} K^{\mp} \pi^{\pm} \pi^0.$$

A semi-reconstruction analysis of the soft pion ($\pi_s^{\pm}$) of the decay

$$D^{*\pm} \rightarrow \pi_s^{\pm} D^0(\bar{D}^0)$$

was also carried out.

2. Experiment

The TOPAZ detector is a general-purpose 4π detector at the TRISTAN e^+e^- collider at KEK.[4] The main detectors include the time-projection chamber (TPC) and the barrel lead-glass calorimeter (BCL). The dE/dx information of the TPC has been used for charged-Kaon-identification.

The data were taken at center-of-mass energies ($\sqrt{s}$) ranging from 52 to 61.4 GeV. The integrated luminosity used in this analysis was $108.4 \pm 0.2 \pm 4.3 \text{pb}^{-1}$; the mean value of $\sqrt{s}$ was 57.95GeV. According to the TOPAZ standard selection criteria,[5] a total of 12696 hadronic events was selected.

The charged tracks used for the full-reconstruction were selected as follows: (1) the number of degrees of freedom in the track fitting be ≥ 3; (2) the transverse momentum (P_{XY}) be greater than 0.2 GeV/c; and (3) the closest approach to the beam axis (Z-axis) be less than 2 cm in the XY-plane and less than 4 cm in the Z-direction. Using these tracks, the event vertices were calculated: (4) those tracks with the closest approach to the event vertex greater than 1.5 cm in the Z-direction were removed. Finally, a vertex constraint fit to the interaction point was carried out for each track. The momentum resolution of this fit was measured to be $\sigma_{P_{XY}}/P_{XY} \sim \sqrt{1 + P_{XY}^2(GeV/c)^2}$ % by $e^+e^- \rightarrow \mu^+\mu^-$ and cosmic $\mu^{\pm}$ events.[4] For a semi-reconstruction analysis of $\pi_s^{\pm}$, cuts of (3) and (4) were loosened to 4 and 3 cm, respectively.

The charged-Kaon-identification was carried out using dE/dx information obtained by the TPC. The dE/dx resolution was obtained to be 4.6%. The following cuts were subjected to the charged Kaon candidate tracks: (1) the number of

dE/dx clusters used in the 65%-truncated mean be greater than 40; (2) χ^2_K for the Kaon assumption be less than 6.6, where the number of degrees of freedom (DOF) is 1, i.e., a 1% confidence level (CL); and (3) χ^2_K be less than χ^2_π+1. Since we considered most of tracks to be $\pi^\pm$ candidates, no dE/dx-cuts were subjected for pion candidates.

The γ-rays were used for jet-axis calculations and π^0 reconstructions. The energy resolution of the γ-rays can be expressed as

$$\frac{\sigma_E}{E} = \sqrt{\left(\frac{8.0}{\sqrt{E(GeV)}}\right)^2 + (1.5)^2} \ \%.$$

For each pair of γ-ray candidates with energies greater than 0.1 GeV, a kinematical fit (1C) assuming the π^0 mass (=0.135 GeV/c^2) was applied. These, with $\chi^2_{\pi^0}$ being less than 6.6 (DOF=1, i.e., 1%CL), were considered to be π^0 candidates.

For a semi-reconstruction analysis, we calculated the jet-axes. We used tracks with momenta greater than 2 GeV/c, and clusters with energies greater than 1 GeV, and not associated to charged tracks. In order to calculate the jet-axes of the events, we used an invariant-mass algorithm,[6] in which particles are merged together in an iterative way if their invariant mass is less than 5 GeV/c^2.

3. Forward-backword asymmetry

The forward-backward asymmetry was measured by exclusive reconstructions of the two decay modes of D^0s and in terms of the inclusive transverse momenta (P_T) of soft $\pi^\pm$s with respect to the jet-axes.

3.1. $D^{*\pm} \to \pi^\pm D^0(\bar{D}^0) \to \pi^\pm K^\mp \pi^\pm$

For every opposite-sign $K^\mp\pi^\pm$ combination, we required the invariant mass to be between 1.4 and 2.2 GeV/c^2; a kinematical constraint fit to the D^0-mass (1.8654 GeV/c^2) (1C-fit) was also employed. For $K^\mp\pi^\pm$-pairs with a χ^2 less than 6.6, we applied a cut on the absolute value of the cosine of the angle of $K^\mp$ at the $K^\mp\pi^\pm$-rest frame with respect to the thrust axis to be less than 0.8 (decay angle cut), since D^0 meson is a scalar particle. Then, the soft $\pi^\pm$s with momenta less than 2 GeV/c were combined (we hereafter call them "soft pion" or "$\pi^\pm_s$" for simplicity). Finally, a cut on the $D^{*\pm}$ energy fraction ($z = E_{D^*}/E_{beam} \geq 0.4$) was applied, in order to reduce the combinatorial background and to suppress any contribution due to cascade decays from B mesons.

The resulting mass difference ($M_{D^{*\pm}} - M_{D^0}$; we hereafter call it "mass difference" for simplicity) is shown in Fig.1-(a). The histogram comprises the experimental data; the hatched histogram indicates the background obtained by a LUND Monte-Carlo (Jetset 6.3) simulation along with a detector simulation.[7] This Monte-Carlo program was tuned so as to fit the average hadronic events.[8] The background in the higher-mass difference region was fit with the Monte-Carlo calculation. We also carried out various background emulations using real data, such

as soft pions rotated by 180 degrees. The emulated background shape agreed with the experimental data.

3.2. $D^{*\pm} \to \pi^{\pm} D^0(\bar{D^0}) \to \pi^{\pm} K^{\mp} \pi^{\pm} \pi^0$

The $K^{\mp}\pi^{\pm}\gamma\gamma$-combinations with invariant masses between 1.45 and 2.3 GeV/c^2 were fitted by a 2C-kinematical fit (i.e., $M_{\gamma\gamma}$ = 0.135 and $M_{K^{\mp}\pi^{\pm}\gamma\gamma}$=1.8645 GeV/$c^2$, respectively). For combinations with χ^2 less than 9.2 (DOF=2, 1%CL), the same decay-angle cuts for the Kaon were applied. Previous measurements of this decay mode showed that most of them decay via vector and pseudo-scalar decays.[9] We therefore applied invariant mass cuts on $K^{\mp}\pi^{\pm}$, $K^{\mp}\pi^0$, or $\pi^{\pm}\pi^0$ of 0.892±0.100GeV/c^2 (K^{*0}), 0.892±0.100GeV/c^2 ($K^{*\mp}$), or 0.77±0.20GeV/c^2 ($\rho^{\pm}$), respectively. We then applied cuts on the two-body decay angles (θ_V) of the vector mesons at their rest frames with respect to the vector-meson moving directions, i.e., $|\cos(\theta_V)| > 0.5$. In the mass-difference analysis in the case of using high-multiplicity decay, there are typically multiple countings. Even when the lowest momentum particle or cluster in the D^0-decay is misidentified, the mass difference falls almost among the same values as in the case of the correct combination.[10] In order to derive the correct statistical significances for the mass-difference plot, we carried out a weighting method. For each soft pion, if there were more than two D^0 candidates for which the mass differences were smaller than 0.22GeV/c^2, they were counted and the reciprocal of the number of candidates was used as a weighting factor. The correctness of this procedure was verified by a Monte-Carlo simulation.

The resulting mass-difference plots are shown in Fig.1-(b).

3.3. Summary of full-reconstruction

In order to derive the forward-backward asymmetry of charm quark pair production, we added the results of the two- and three-body decays. However, there were duplications of events due to the same process as in multiple counting (described before). We thus carried out the same weighting procedure as described in the previous section, including both two- and three-body D^0 candidates for each soft pion at the same time in order to derive the correct statistical significance of the events. Any entry having a mass-difference less than 0.152 GeV/c^2 was considered to be a $D^{*\pm}$ candidate. The Monte-Carlo backgrounds were subtracted in each $\cos\theta_{D^*}$ binning and the acceptances were corrected. Fig.2 shows the distribution of the cosine of the polar angle obtained by the above-mentioned procedure.

The $D^{*\pm}$ yield was obtained to be $25.2 \pm 10.2(stat.)$ events. In order to derive the $D^{*\pm}$ production cross section, we used the branching ratios of D^0 by the particle data group (PDG).[9] Also, the branching ratio of $D^{*\pm} \to \pi^{\pm} D^0(\bar{D^0})$ was set to be 68.1%, which was recently obtained by CLEO.[11]

The fitting function was $f = 3/8 \cdot \sigma(c \to D^{*\pm})/\sigma_{q\bar{q}} \cdot (1 + \cos^2\theta + 8/3 A_{FB}^c \cos\theta)$; the maximum-likelihood method was used. The best fit gave

$$\sigma(c \to D^{*\pm})/\sigma_{q\bar{q}} = 0.129^{+0.056}_{-0.049} \pm 0.031 \quad \text{and} \quad A_{FB}^c = -0.50^{+0.33}_{-0.29} \pm 0.08.$$

Here, the first error is statistical and the second systematic. The systematic error included the statistics of the Monte-Carlo simulation, the ambiguity of the branching ratios of D and D^* mesons, the ambiguity of the background determinations, and analysis systematics (especially for a dE/dx calibration error). The best-fitted

function and the prediction of the Standard model are also indicated by the solid and dashed curves, respectively, in Fig.2. In order to estimate $\sigma^{theory}(c \to D^{*\pm})$, we used $Br(c \to D^{*\pm}) = 22 \pm 6\%$, which was obtained by the VENUS collaboration.[3]

3.4. Semi-reconstruction of $D^{*\pm} \to \pi^{\pm} D^0(\bar{D}^0)$

We also analyzed the inclusive P_T distribution of soft pions with respect to the jet-axis. The soft pion from $D^{*\pm} \to \pi_s^{\pm} D^0(\bar{D}^0)$ has a P_T lower than 0.039 GeV/c with respect to the D^* direction, where the D^* direction can be approximated by the jet-axis.[12] The definition of the jet-axes was mentioned in the previous chapter.

The soft pions were required to have momenta between 0.8 and 2.0 GeV/c^2. In order to reject the e^+ and e^- tracks originating from a γ conversion, the tracks with a $\chi^2_{e\pm}$(dE/dx) less than 2.7 were removed.

The P_T distributions of the soft pions are shown in Figs 3 (a) and (b), for the forward and backward pions, respectively. The fitting function used was

$$f({P_T}^2) = \frac{\alpha}{1 + \frac{({P_T}^2)^\gamma}{\beta}}.$$

The shape parameters of the signal were fitted via a Monte-Carlo study. The signal entry and the background shape parameters were fitted with the experimental data. There is a significant excess of entries in the low-P_T region, especially for backward-going pions. We obtained excesses of 121 ± 45 and 336 ± 49 events in the forward and backward directions, respectively. Using an acceptance correction based on

the Monte-Carlo simulation, we obtained

$$\sigma(c \to D^{*\pm})/\sigma_{q\bar{q}} = 0.114 \pm 0.017 \pm 0.020 \quad \text{and} \quad A_{FB}^c = -0.49 \pm 0.15 \pm 0.08.$$

Both the full- and semi-reconstruction results were consistent with each other.

3.5. Combined result

Combining both the full- and semi-reconstruction results, we obtained average values of

$$\sigma(c \to D^{*\pm})/\sigma_{q\bar{q}} = 0.116 \pm 0.016 \pm 0.017 \quad (0.141 \pm 0.038)$$

$$\text{and} \quad A_{FB}^c = -0.49^{+0.14}_{-0.13} \pm 0.06 \quad (-0.47),$$

which are consistent with the prediction of the Standard model (values given in parentheses). The forward-backward asymmetry is shown in Fig.4, together with the other experimental data at various $\sqrt{s}$.[2] The solid line is a prediction of the Standard model with $\sin^2\theta_W$=0.2325 and M_Z=91.173 GeV/c^2.

From the cross section, we obtained $Br(c \to D^{*\pm}) = 0.181 \pm 0.025 \pm 0.026$, which is consistent with the VENUS results[3] and slightly lower than those of ALEPH.[13] Assuming the Standard model with the axial vector coupling constant of the electron being -1, we obtained the axial vector coupling constant of the charm quark to be $a_c = 1.07^{+0.47+0.19}_{-0.36-0.16}$, which is consistent with unity.

4. Conclusion

We measured the forward-backward charge asymmetry of $D^{*\pm}$ production using the TOPAZ detector at the TRISTAN e^+e^- collider at an average center-of-mass energy of 57.95GeV and an integrated luminosity of $108.4 \pm 0.2 \pm 4.3\text{pb}^{-1}$. In order to derive the $D^{*\pm}$ production cross section and the forward-backward asymmetry, we used exclusive reconstructions of two-decay chains and inclusive P_T distributions for soft $\pi^{\pm}$s from the $D^{*\pm}$ decay. The measured asymmetry was $A_{FB}^c = -0.49^{+0.14}_{-0.13} \pm 0.06$, consistent with the Standard model. The axial-vector coupling constant of the charm quark was obtained to be $a_c = 1.07^{+0.47+0.19}_{-0.36-0.16}$ by assuming that the axial-vector coupling constant of the electron is -1. The cross section was obtained to be $\sigma(c \to D^{*\pm})/\sigma_{q\bar{q}} = 0.116 \pm 0.016 \pm 0.017$. From this cross section, we obtained $Br(c \to D^{*\pm}) = 0.181 \pm 0.025 \pm 0.026$.

Acknowledgements: We thank the TRISTAN accelerator physicists, engineers and staff for the successful operation of TRISTAN. We also thank all of the engineers and technicians at KEK as well as the collaborating institutions: H. Inoue, K. Shiino, M. Tanaka, K. Tsukada, N. Ujiie, and H. Yamaoka.

REFERENCES

1. S. Weinberg, Phys. Rev. Lett. 19 (1967) 1264; A. Salam, in: Elementary particle theory; relativistic group and analyticity, Nobel Symp. No. 8, ed. N. Svartholm (Almqvist and Wiksells, Stockholm, 1968) p. 361; S. L. Glashow, Nucl. Phys. 22 (1961) 1579.

2. M. Althoff et al., Phys. Lett. B 126 (1983) 493; W. Braunschweig et al., Z. Phys. C 44 (1989) 365; W. Bartel et al., Phys. Lett. B 146 (1984) 121; F. Ould-Saada et al., Z. Phys. C 44 (1989) 567; H. Aihara et al., Phys. Rev. D 34 (1986) 1945; M. Derrick et al., Phys. Lett. B 146 (1984) 261; P. Baringer et al., Phys. Lett. B 206 (1988) 551; H. Aihara et al., Z. Phys. C 27 (1985) 39; H. Aihara et al., Phys. Rev. D 31 (1985) 2719; M. Althoff et al., Phys. Lett. B 146 (1984) 443; H. J. Behrend et al., Z. Phys. C 47 (1990) 333; E. Elsen et al., Z. Phys. C 46 (1990) 349; B. Adeva et al., Phys. Rep. 109 (1984) 133; D. Decamp et al., Phys. Lett. B 263 (1991) 325; O. Adriani et al., Phys. Lett. B 292 (1992) 454.

3. A. Okamoto et al., Phys. Lett. B 278 (1992) 393; F. Hinode et al., KEK Preprint 92-194, to be published in Phys. Lett. B.

4. R. Enomoto et al., Nucl. Instrum. Methods A 269 (1988) 507; A. Imanishi et al., Nucl. Instrum. Methods A 269 (1988) 513; T. Kamae et al., Nucl. Instrum. Methods A 252 (1986) 423; A. Yamamoto et al., Jpn. J. Appl. Phys. Lett. 25 (1986) L440; S. Kawabata et al., Nucl. Instrum. Methods A 270 (1988) 11; J. Fujimoto et al., Nucl. Instrum. Methods A 256 (1987) 449; S. Noguchi et al., Nucl. Instrum. Methods A 271 (1988) 404; K.Fujii et al., Nucl. Instrum. Methods A 264 (1988) 297.

5. I. Adachi et al., Phys. Lett. B 255 (1991) 613.

6. W. Bartel et al., Z. Phys. C33 (1986) 23.

7. T. Sjostrand, Comput. Phys. Commun. 39 (1986) 347; T. Sjostrand and M. Bengtsson, Comput. Phys. Commun. 43 (1987) 367.

8. I. Adachi et al., Phys. Lett. B227 (1989) 495.

9. Particle Data Group, Phys. Rev. D45, No.11, Part II (1992).

10. H. Aihara et al., Phys. Rev. Lett. 53 (1984) 2465; R. Enomoto, UT-HE-86/1, Univ. of Tokyo preprint (1986), unpublished.

11. F. Bulter et al., Phys. Rev. Lett. 69 (1992) 2041.

12. P. Baringer et al., Phys. Lett. B206 (1988) 551.

13. D. Decamp et al., Phys. Lett. B266 (1991) 218.

FIGURE CAPTIONS

1) Mass differences of the decay :(a) $D^{*\pm} \to \pi^{\pm} D^0(\bar{D}^0) \to \pi^{\pm} K^{\mp} \pi^{\pm}$(left scale) and (b) $D^{*\pm} \to \pi^{\pm} D^0(\bar{D}^0) \to \pi^{\pm} K^{\mp} \pi^{\pm} \pi^0$(right scale). The histogram is based on the experimental data, and the hatched histogram is a Monte-Carlo simulation.

2) Angular distribution of the $D^{*\pm}$ events. Background subtraction and an acceptance correction were carried out. The solid curve is the best fit and the dashed curve is the prediction of the Standard model.

3) Inclusive P_T^2 distribution of $\pi^{\pm}$s for the decay $D^{*\pm} \to \pi^{\pm} D^0(\bar{D}^0)$: (a) forward events and (b) backward events. The histogram is based on the experimental data, the lines are the best-fitted functions, and the dots with error bars are background-subtracted signals.

4) Forward-backward asymmetry (A_{FB}^c) versus $\sqrt{s}$, together with other experimental results.[2]

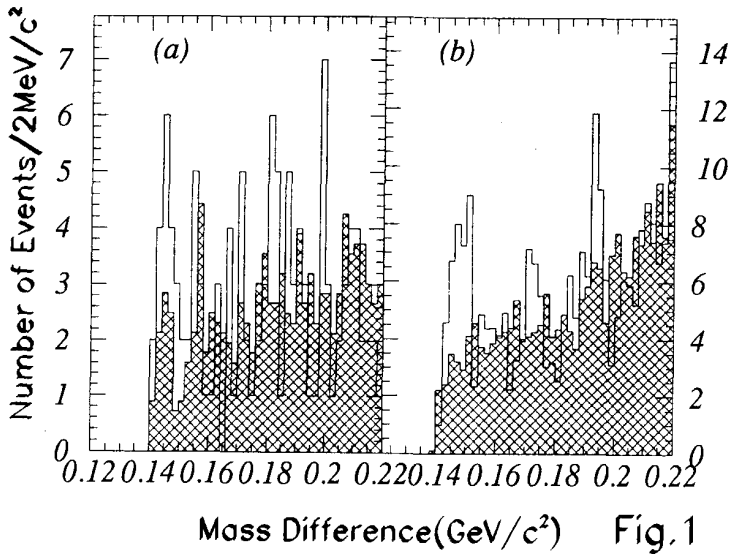

Fig.1

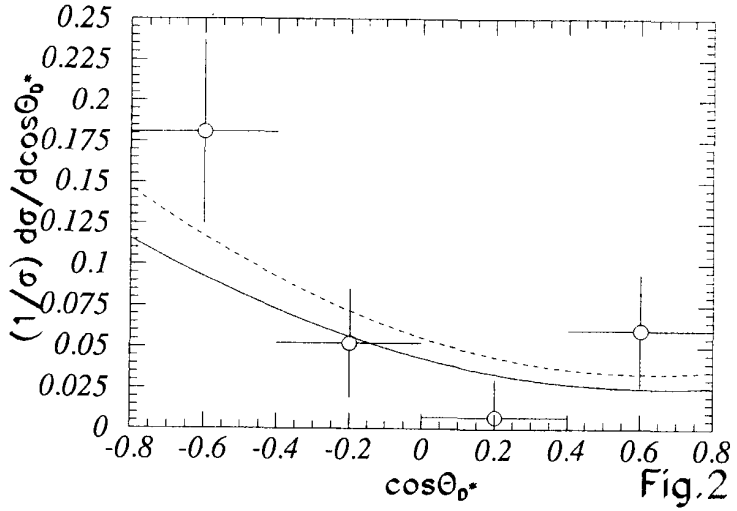

Fig.2

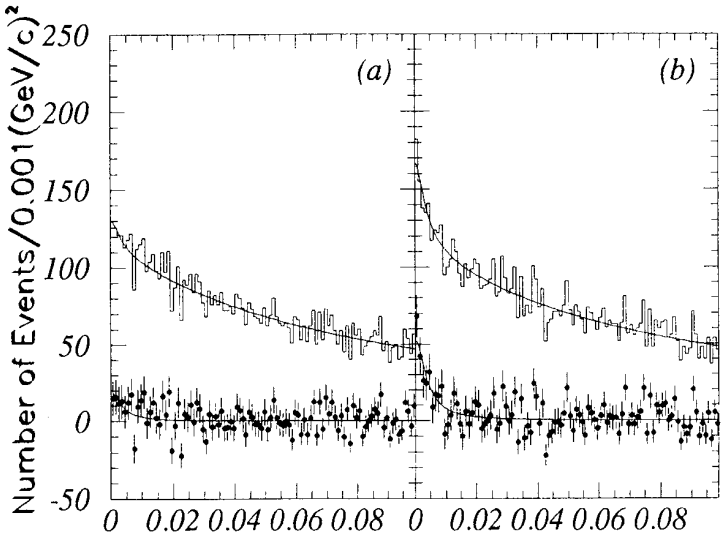
(a)
(b)
Number of Events/0.001(GeV/c)²
250
200
150
100
50
0
-50
0 0.02 0.04 0.06 0.08 0 0.02 0.04 0.06 0.08
P_t²(GeV/c)²

Fig.3

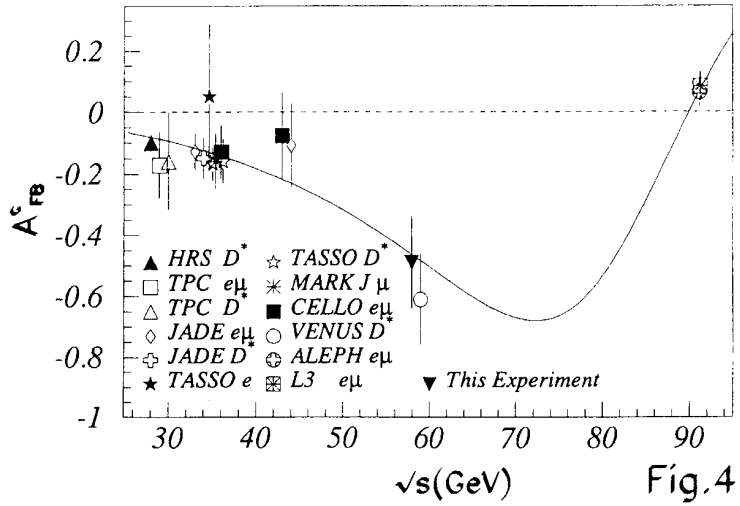
A^c_FB
0.2
0
-0.2
-0.4
-0.6
-0.8
-1
HRS D*
TPC eμ
TPC D*
JADE eμ
JADE D*
TASSO e
TASSO D*
MARK J μ
CELLO eμ
VENUS D*
ALEPH eμ
L3 eμ
This Experiment
30 40 50 60 70 80 90
√s(GeV)

Fig.4